WILEY

Development of the multispectral UV polarization reflectance imaging system (MUPRIS) for in situ monitoring of the UV protection efficacy of sunscreen on human skin

Ken Nishino[1] 🆔 | Yasushi Haryu[2] | Ayui Kinoshita[3] | Shigeki Nakauchi[3]

[1]Makeup Products Research, Kao Corporation, Odawara, Kanagawa, Japan

[2]Skin Care Products Research, Kao Corporation, Odawara, Kanagawa, Japan

[3]Department of Computer Science and Engineering, Toyohashi University of Technology, Toyohashi, Aichi, Japan

Correspondence
Ken Nishino, Makeup Products Research, Kao Corporation, Odawara, Kanagawa, Japan.
Email: nishino.ken@kao.com

Abstract

Background: Protection of the human skin from ultraviolet (UV) damage is one of the main issues in dermatology and cosmetology. The UV protection efficacy (UVPE) of the sunscreen film is decreased by sweat, sebum, and friction during the day. However, the technical relationship between the UVPE evaluated in a laboratory and the actual protection in daily use has not been clarified, because the UVPE measurement method in real-life setting has not been established. This study aimed to develop a novel UVPE evaluation system that allows in situ monitoring of the UVPE in real-life activities.

Methods: The multispectral UV polarization reflectance imaging system (MUPRIS) and a UVPE estimation algorithm were developed. The diffuse reflectance spectra were measured for a total of 48 sunscreen materials that were applied on 59 subjects. The UVPEs estimated from the diffuse reflectance spectra were compared with the in vivo SPFs. Finally, the UVPE before and after a marine leisure activity was evaluated using the MUPRIS as the practical use test.

Results: Compared with the conventional UV camera, the MUPRIS could visualize the applied sunscreen more clearly and showed good UVPE estimation accuracy (correlation coefficient for in vivo SPF, 0.82). In the practical use test, the degradation of the UVPE during a marine leisure activity was quantitatively monitored and was validated by the actual occurrence of sunburn.

Conclusions: A novel in situ UVPE monitoring tool had been successfully developed. It can strongly support the development of innovative sunscreen products that can perfectly protect customers against UV irradiation in real-life situation.

KEYWORDS
multispectral imaging, SPF, sunburn, sunscreen, ultraviolet, UV protection efficacy

1 | INTRODUCTION

Living body tissues have high reactivity to ultraviolet (UV) radiation that is present in natural sunlight. Therefore, protecting the human skin from UV damage is one of the main issues in dermatology and cosmetology,[1] particularly regarding the prevention of cancer, premature aging, and pigmentation changes.[2-4] Sunscreen is often used to protect the human skin from UV damage, and the most popular index of UV protection efficacy (UVPE) for sunscreen products is the sun protection factor (SPF) value, which is prominently displayed on products offered for sale. Because SPF is a ratio calculated from the energies required to induce a minimum erythema response with and without in vivo sunscreen, it certainly shows the protection efficacy for sunburn.[5] However, several researchers have reported that the SPF can sometimes fail to accurately capture the protection efficacy in real-life situations.[6] Degradation of the UVPE by extrinsic factors, such as water, sweat, and friction, was considered as one of the major causes of the potentially significant difference between a stated SPF and the actual protection efficacy in real-life situations.[7-9] In fact, the water resistance efficacy testing method was established based on an in vivo SPF test and is now widely used for water-resistant claims.[7] In addition, the UVPE degradation effects of clothing, sweating, and bathing were studied based on the in vivo SPF test method.[8,9] However, although extrinsic factors are well known to decrease the UVPE, the technical relationship between the laboratory effectiveness of sunscreen and the actual protection that it provides in daily use has not been clarified. A rigorous understanding on how the UVPE can be degraded in real-life situations would be very helpful for both customers and companies that produce sunscreens. Our goal in this study was to improve this current situation.

To investigate UVPE degradation in the real-life setting, a quantitative UVPE monitoring technology that can capture in situ the site and time of degradation should be developed. In other words, a quantitative and spatiotemporal measurement method is required. As described above, the traditional in vivo SPF test method had been applied for the evaluation of UVPE degradation; this method entails the use of UV radiation to generate sunburn on a local area on the skin and evaluating for erythema the next day. Although this method can quantitatively measure the UVPE against sunburn, it is unsuitable for in situ evaluation for several reasons, including (a) problems on defining and measuring the affected area precisely; (b) invasive nature of this approach; and (c) the time required.

There are several reports for the quantitative evaluation of the sunscreen membrane. Some studies demonstrated that the thickness of applied sunscreen can be quantified by swab collection or tape stripping.[10-13] However, these methods are not suitable for temporal measurement because removal of the applied sunscreen can be destructive. Some studies applied the fluorescent measurement technique to quantify sunscreen thickness based on the fluorescent light of the contained ingredients or the human skin.[14-17] Although these approaches may allow noninvasive, nondestructive, and temporal measurements, these only work in laboratory studies.

On the other hand, because the invasive nature of the in vivo SPF method is troublesome, the development of an alternative approach had been studied both in vivo and in vitro.[19-23] Diffuse reflectance spectroscopy (DRS) techniques provide quantitative evaluation of in vivo SPF without any invasive process.[21-23] Reble et al proposed a method to estimate the in vivo SPF by distance-dependent DRS, and they applied it on five test materials that had an SPF range of 16-73.2.[21] Ruvolo et al proposed a new in vivo SPF assessment method that combined the human skin diffuse reflectance spectra and the in vitro transmittance spectra of sunscreen material.[22] Rohr et al demonstrated that hybrid diffuse reflectance spectroscopy (HDRS) provided great SPF estimation accuracy for a huge variety of sunscreen materials (R^2 = 0.973 for 80 materials in a wide formulation).[23] However, because these methods require contact examination of a particular skin site, in situ spatiotemporal evaluation is difficult.

The use of a UV camera is an alternative and strong qualitative tool for determining the effectiveness of sunscreen, because it readily allows noninvasive evaluation over time and in a variety of settings.[24,25] In a UV image, regions where sunscreen had been applied are significantly darker than bare skin because sunscreen absorbs UV light. Unfortunately, the conventional UV cameras used for the qualitative evaluation of the UVPE have the major technical drawback of not being able to distinguish between a low-UVPE region and specular light. In this technique, although the area with low UVPE is visualized as bright, specular light is also shown as bright, without regard to the UVPE. Moreover, conventional UV cameras are most sensitive to the UVA region, but the reactivity to erythema according to the action spectrum is significantly high in the UVB range. Therefore, measuring the UVA range by conventional UV camera is unsuitable for actual estimation of the UVPE.

This study aimed to develop a novel evaluation method for resolving these problems. To proceed, we employed a multispectral imaging technique that can measure an image with spectral data for each pixel. This multispectral imaging device designed for the UVB-to-UVA wavelength range could simultaneously provide spatiotemporal and quantitative measurements that are similar to those provided by a UV camera and a DRS system, respectively. In addition, a cross-polarization technique can be applied to this system to eliminate the specular reflection.

In this study, we realized a quantitative and spatiotemporal UVPE evaluation system by developing a multispectral UV polarization reflectance imaging system (MUPRIS) together with a UVPE estimation algorithm. We then applied this system for in situ monitoring, in the context of marine leisure activities, to investigate the de facto impact of the factors that reduce UVPE in a practical setting.

2 | MATERIALS AND METHODS

2.1 | Multispectral UV polarization reflectance imaging system

In order to satisfy real-life situation monitoring of the UVPE, the novel MUPRIS was developed to capture a diffuse reflectance multispectral
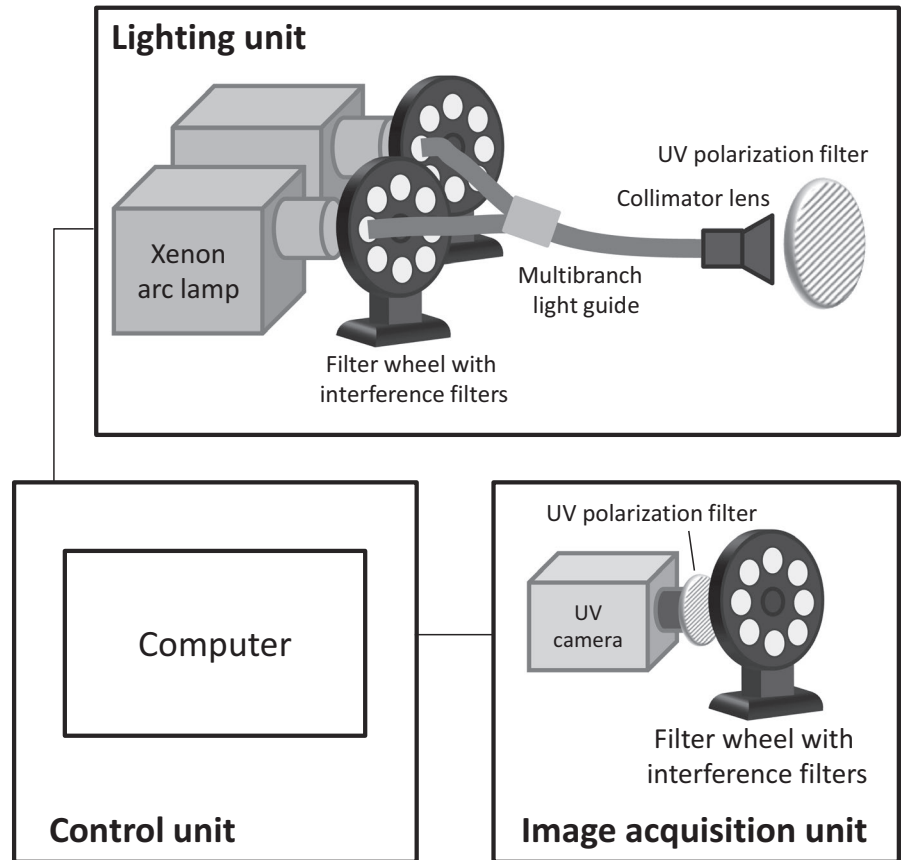
FIGURE 1 The configuration of the multispectral ultraviolet (UV) polarization reflectance imaging system (MUPRIS)

image in the UVA-to-UVB wavelength range for wide test sites (about 30 × 30 cm) with high measurement accuracy. The configuration of the MUPRIS is illustrated in Figure 1. This system comprised a control unit, a lighting unit, and an image acquisition unit. This was a "dual spectral filtering system" that was similar to the double monochromatic system adopted in the HDRS.[22,23] The UV spectral interference filter sets in the same wavelength range (310-380 nm in 10-nm steps) were mounted on both the light unit and the image acquisition unit. The spectral filtering on the light source can decrease the total UV exposure (ie, UV damage) of the test site, and the filtering on the camera can eliminate the fluorescent light emitted from the test site. In addition, UV polarization filters were mounted on both units to eliminate the specular light component by cross-polarization. This system design allowed accurate noncontact, noninvasive, and nondestructive UV diffuse reflection imaging. The control unit was designed to allow synchronous rotation of all filter wheels and to capture a UV image for each wavelength. The captured images for all wavelengths were constructed in a multispectral image that had a UV spectrum for each pixel. The diffuse reflectance multispectral image was defined as the ratio between the multispectral images of a target and a baseline. The details of the measurement and the computation procedures are described in the next section.

In this study, we used two xenon arc lamps (MAX-303, Asahi Spectra Co., Japan) with a multibranch light guide and a collimator lens as the lighting unit. The UV camera used was BU56-DUV (BITRAN CORPORATION, Japan), which had spectral sensitivity across the entire UVB-to-UVA wavelength range. The image resolution was

680 × 512 pixels. The UV band-pass filters (310-380 nm in 10-nm steps; Asahi Spectra Co., Japan) were mounted on all filter wheels. The control unit was a conventional laptop computer that had USB ports.

To confirm the effect of cross-polarization, the 360-nm UV images of a human face, half of which had a conventional sunscreen applied, were captured with and without cross-polarization. To demonstrate the benefit of UVB-to-UVA measurement, the skin of a human back on which four different sunscreens were applied was imaged at 320 and 380 nm. To assess the erythema risk of the subjects, the erythema-weighted UV dose measured by the calibrated UV Radiometer PMA2100 was compared with the multispectral image measurements of the entire wavelength.

2.2 | UVPE evaluation method

The following steps describe the flow of UVPE measurement by the MUPRIS (also see Figure 2). Here, x and y represent the vertical and horizontal positions in the image, respectively, and the λ represents the wavelength.

Step 1: Measurement of the multispectral image of the baseline (without test material) $S_b(x, y, \lambda)$.

Step 2: Measurement of the multispectral image of the target (with test material) $S_t(x, y, \lambda)$.

Step 3: Computation of the relative diffuse reflectance multispectral image $R_r(x, y, \lambda)$ from S_b and S_t.
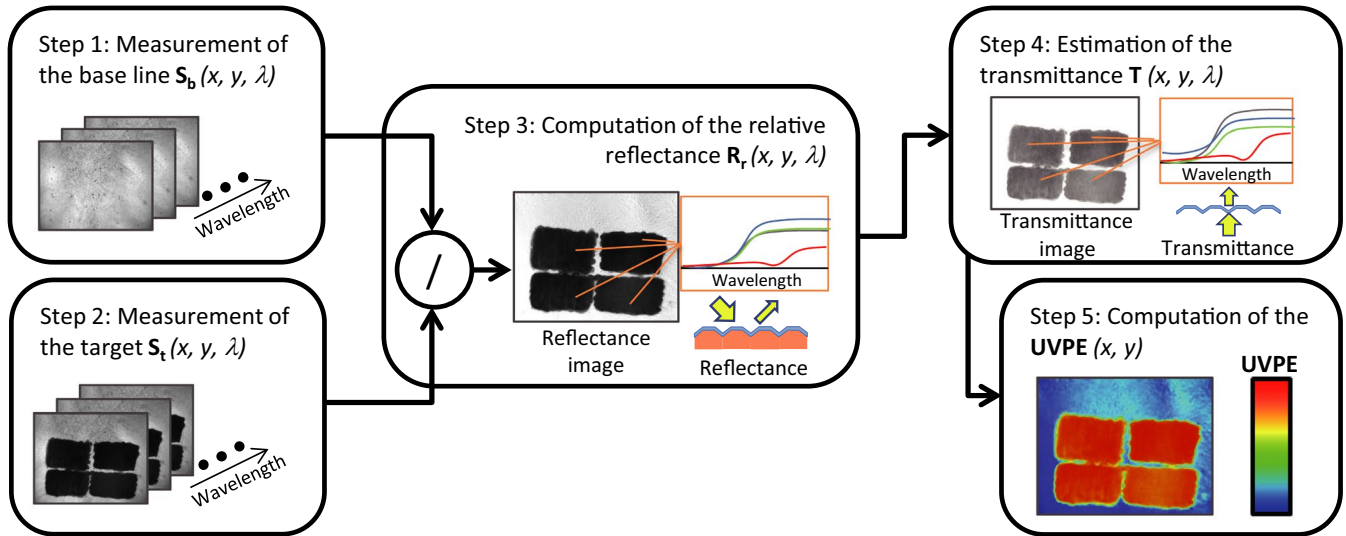
FIGURE 2 Process of UV protection efficacy (UVPE) evaluation by the MUPRIS [Colour figure can be viewed at wileyonlinelibrary.com]

Step 4: Estimation of the transmittance spectra of the sunscreen membrane $T(x, y, \lambda)$ from R_r.

Step 5: Computation of the pixel by pixel $UVPE(x, y)$ from T.

In steps 1 and 2, the test sites can be measured by the MUPRIS. In step 3, the diffuse reflectance multispectral image $R_r(x, y, \lambda)$ was defined as the relative reflectance between S_b and S_t. With this process, the unknown factors in S_b and S_t, including the spatial variation and spectral property of the irradiance $I(x, y, \lambda)$ and the spectral sensitivity of the UV camera $C(\lambda)$, were removed. The ratio of the diffuse reflectance with the test material $R_b(x, y, \lambda)$ and that without the test material $R_t(x, y, \lambda)$ was obtained as $R_r(x, y, \lambda)$.

$$R_r(x,y,\lambda) = \frac{S_t(x,y,\lambda)}{S_b(x,y,\lambda)} = \frac{I(x,y,\lambda)\, R_t(x,y,\lambda)\, C(\lambda)}{I(x,y,\lambda)\, R_s(x,y,\lambda)\, C(\lambda)} = \frac{R_t(x,y,\lambda)}{R_b(x,y,\lambda)} \quad (1)$$

In step 4, the transmittance of the applied test material $T(x, y, \lambda)$ was estimated by the transmittance estimation function f_T. The estimated transmittance was defined as $T'(x, y, \lambda)$. Finally, UVPE was evaluated based on the equation of in vitro SPF calculation in step 5.[8]

$$T'(x,y,\lambda) = f_T\left(R_r(x,y,\lambda)\right) \quad (2)$$

$$UVPE(x,y) = \frac{\sum_{310}^{380} E(\lambda)\, I_S(\lambda)}{\sum_{310}^{380} T'(x,y,\lambda)\, E(\lambda)\, I_S(\lambda)} \quad (3)$$

where $E(\lambda)$ represented erythema spectral effectiveness and $I_S(\lambda)$ represented spectral irradiance of sunlight.

Therefore, the first problem setting of UVPE evaluation in a real-life situation can be replaced by a new problem setting of designing the transmittance estimation function $T'(\lambda) = f_T(R_r(\lambda))$. In this study, we prepared a training dataset that comprised the relative reflectance spectra $R_{ri}(\lambda)$ ($i = 1,2,....,N$); in vivo SPF of the test materials SPF_i; and the theoretical transmittance spectra $T_i(\lambda)$ ($i = 1,2,....,N$) in

order to establish f_T. For this dataset, N was the number of the reflectance spectra. The details of the training dataset measurement are described in Section 2.31. Using the training dataset, the accuracy of UVPE estimation by the three different transmittance estimation functions [ie, Equations 4-6] was evaluated. The standard error of prediction (SEP) defined in Equation 7 was used to evaluate their estimation accuracies. Here, the $UVPE_i$ represented the training dataset estimated UVPE, which was calculated from the estimated transmittance $T'_i(\lambda)$ obtained by Equation (4) and the UVPE calculation Equation (3).

$$T'_i(\lambda) = f_T\left(R_{ri}(\lambda)\right) = \begin{cases} \sqrt{R_{ri}(\lambda)} \\ \{R_{ri}(\lambda)\}^{\gamma_b} \\ \{R_{ri}(\lambda)\}^{\gamma_{si}(\lambda)} \end{cases} \quad (4)$$

$$SEP = \sqrt{\frac{\sum_i (UVPE_i - SPF_i)^2}{N}} \quad (5)$$

The optical models corresponding to the estimation equations are described in Figure 3. Equation (4) was similar to the transmittance estimation function described in an earlier study[21-23] and assumed that the sunscreen membrane was a homogenous layer on the skin (Figure 3A). In this case, when an incident light went through the sunscreen layer two times, the light path length (d in Figure 3) was 2 and the transmittance can be estimated by the square root of the relative reflectance. The other two equations were designed to account for the changes in the light path length (d) by penetration of the sunscreen membrane and the scattering effect caused by the UV scattering material in the sunscreen. In Equation (4), the gamma correction parameter γ_b was introduced for the unknown light path length. In this study, γ_b was determined to minimize the SEP in Equation (5). The scattering effect of the test material is determined

$$R_r(\lambda) = T^2(\lambda) \qquad R_r(\lambda) = T^d(\lambda) \qquad R_r(\lambda) = T^{d(\lambda)}(\lambda)$$

Sunscreen	Sunscreen	Sunscreen
Skin	Skin Penetration	Scattering material
		Skin Penetration
	d: Average light path length	$d(\lambda)$: Wavelength depending average light path length
(a) Simple optical model (Equation 4)	(b) With penetration (Equation 5)	(c) With scattering (Equation 6)
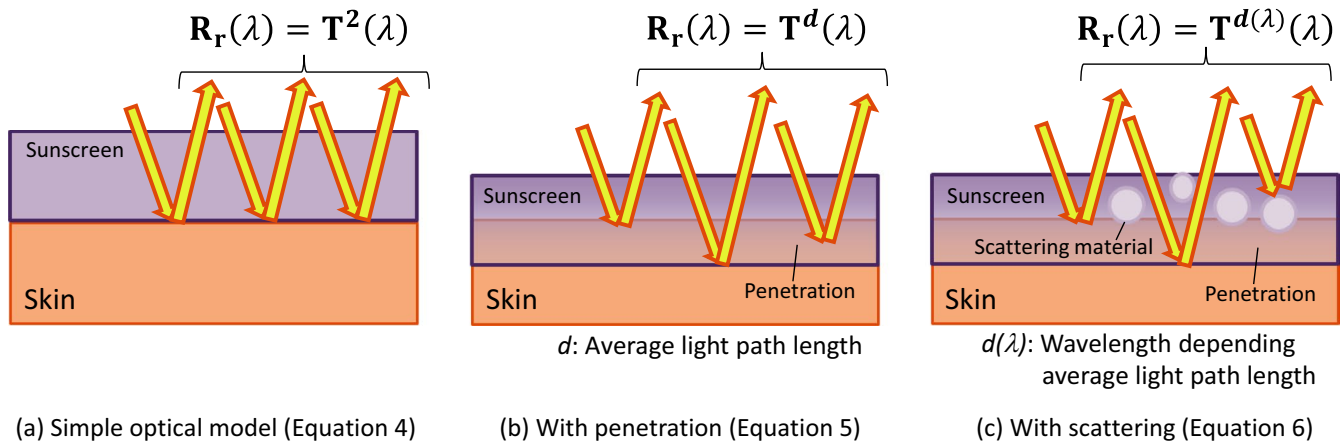
FIGURE 3 Optical models for the transmittance estimation equations [Colour figure can be viewed at wileyonlinelibrary.com]

in Equation (4). The newly introduced gamma correction parameters vector $\gamma_{si}(\lambda)$ was used to correct the estimation error caused by the scattering effect of the wavelength. As shown below, this parameter was defined as the scatter/ transmission ratio spectrum that was computed from the premeasured in vitro scattering and transmittance spectra. The measurement procedure is described in Section 2.31. Here, $a(\lambda)$, $b(\lambda)$, $c(\lambda)$, and $\beta(\lambda)$ represented the correction coefficients vectors, which were determined to minimize the transmittance estimation error that was defined as Equation (7) for the training dataset. The optimal parameters were found using an optimization function "fminsearch" in MATLAB 2017b.

$$\gamma_{Si}(\lambda) = a(\lambda) \left(S_{Ci}(\lambda) - b(\lambda) \right)^{\beta(\lambda)} + c(\lambda) \qquad (6)$$

$$e(\lambda) = \sum_i \left(\frac{1}{T_i(\lambda)} - \frac{1}{T_i'(\lambda)} \right)^2 \qquad (7)$$

2.3 | Training dataset measurement

To establish the UVPE evaluation method described in Section 2.2, we measured the relative reflectance spectra, theoretical transmittance spectra, scatter/transmission ratio spectra, and in vivo SPF as the training dataset. SPF-labeled products, including cosmetics, available in the market and UV protection materials prepared in our laboratory, were used as the test materialsTable 1). We selected a wide variety of sunscreen formula that contained inorganic and organic ingredients or both UV filters.

These in vivo SPFs were measured by an external institute, in accordance with the ISO 24444:2010. As described in Table 1, the number of subjects for the in vivo SPF calculations ranged from 3 to 12. The relative reflectance dataset $R_{ri}(\lambda)$ was measured by the MUPRIS. A total of 59 subjects (39 men and 20 women) were participated in our study and signed informed consent forms after understanding the nature of the investigation. This experiment had been approved by the ethical review board of Kao Corporation.

Three or four test sites (6 × 6 cm for each) were prepared on the back of each subject. At this point, a UV multispectral image without the test materials $S_b(x, y, \lambda)$ was measured. Next, the test materials were applied with a density of 2 mg/cm². Finally, a UV multispectral image of the test material $S_t(x, y, \lambda)$ was measured after drying for 15 minutes. The relative reflectance spectral image $R_r(x, y, \lambda)$ was computed from the measured multispectral images, and the average reflectance spectrum of the test material applied was computed as $R_{ri}(\lambda)$. As described in Table 1, in the experiment for the relative reflectance measurement, 3 to 6 subjects were examined for each test materials. In total, 201 relative reflectance spectra were measured. This experiment was conducted between June 2016 and June 2017.

In vitro transmittance spectra $T_{Pi}(\lambda)$ and scattering spectra $S_{Si}(\lambda)$ were measured for computation of the theoretical transmittance and scatter/ transmission ratio spectra. The transmittance measurement device was the SPF analyzer UV1000S, and the scattering measurement device was the MUPRIS. PMMA plate (Helio plate HD6) was used as the measurement substrate. The geometry of the scattering spectra measurement is described in Figure 4.

The scattering spectrum can be measured by reflectance spectrum measurement in this geometry, because the light transmitted by the substrate can be absorbed by the black background material. First, the transmittance spectrum and scattering spectral image of the PMMA plate without the test material were measured as the baseline. Next, 1.3 mg/cm² of the test material was applied to the PMMA plate and was dried for 15 minutes. Thereafter, the average of the transmittance spectra measured for five different positions was calculated. Here, the wavelength range of the transmittance measurement was 290-400 nm in 1-nm steps. Next, the reflectance spectral image was measured by the MUPRIS. The ratio of the reflectance spectral image to the baseline was computed, and the average spectrum of the PMMA plate region was extracted. Three PMMA plates were examined for each test material, and the average spectra of three transmittance and scattering spectra were calculated as $T_{Pi}(\lambda)$ and $S_{Si}(\lambda)$, respectively. Then, the scatter/ transmission ratio spectrum $S_{Ci}(\lambda)$ and the theoretical transmittance spectrum $T_i(\lambda)$ can be obtained by Equations 8 and 9.

TABLE 1 Test materials

| Sample # | Form | Category | Sold in Market | UV filter | | n | |
				Organic	Inorganic	In vivo SPF	MUPRIS
1	O/W	Sunscreen	x	x	x	12	5
2	O/W	Sunscreen	x	x	x	3	6
3	O/W	Sunscreen	x	x	x	3	6
4	O/W	Sunscreen	x	x		3	6
5	W/O	Makeup foundation	x	x	x	3	6
6	W/O	Makeup primer	x	x	x	3	6
7	O/W	Makeup primer	x	x	x	3	6
8	W/O	Sunscreen			x	3	6
9	O/W	Sunscreen		x		3	6
10	O/W	Sunscreen		x		3	6
11	O/W	Sunscreen		x		3	6
12	O/W	Sunscreen	x	x		10	6
13	O/W	Sunscreen		x	x	3	6
14	W/O	Sunscreen	x	x	x	3	6
15	O/W	Sunscreen	x	x	x	3	6
16	W/O	Sunscreen	x	x	x	3	6
17	W/O	Makeup foundation	x	x	x	5	6
18	Solid oil	Makeup foundation	x	x	x	5	6
19	W/O	Sunscreen	x	x	x	10	3
20	O/W	BB cream	x	x	x	11	3
21	O/W	Sunscreen		x	x	5	3
22	O/W	Sunscreen	x	x	x	10	3
23	O/W	Sunscreen	x	x	x	3	5
24	O/W	Sunscreen	x	x	x	3	3
25	O/W	Sunscreen	x	x	x	3	4
26	O/W	Sunscreen	x	x		3	3
27	O/W	Sunscreen	x	x		3	3
28	O/W	Sunscreen	x	x	x	11	3
29	W/O	Sunscreen	x	x	x	12	3
30	W/O	Sunscreen	x		x	10	3
31	W/O	Sunscreen	x		x	11	3
32	O/W	Sunscreen		x	x	3	3
33	O/W	Sunscreen		x	x	5	3
34	O/W	Sunscreen		x	x	3	3
35	O/W	Sunscreen	x	x	x	3	3
36	W/O	Sunscreen	x		x	3	3
37	O/W	BB cream	x	x	x	3	3
38	O/W	Sunscreen	x	x	x	3	4
39	W/O	Sunscreen	x		x	3	3
40	O/W	Sunscreen	x	x		3	3
41	W/O	Sunscreen			x	3	3
42	W/O	Sunscreen			x	3	3
43	W/O	Sunscreen	x	x	x	3	3

TABLE 1 (Continued)

| Sample # | Form | Category | Sold in Market | UV filter | | n | |
				Organic	Inorganic	In vivo SPF	MUPRIS
44	O/W	Sunscreen	x	x		3	3
45	W/O	Sunscreen	x	x	x	3	3
46	O/W	Sunscreen	x	x		3	3
47	W/O	Sunscreen	x	x	x	3	3
48	W/O	Sunscreen	x		x	3	3

$$\mathbf{S_{Ci}}(\lambda) = \mathbf{S_{Si}}(\lambda) / \mathbf{T_{Pi}}(\lambda) \qquad (8)$$

$$\mathbf{T_i}(\lambda) = c_{ti} \mathbf{T_{Pi}}(\lambda) \qquad (9)$$

Here, c_{ti} was the coefficient to adjust $\mathbf{T_{Pi}}(\lambda)$ to match the in vitro and in vivo SPF. Therefore, the in vitro SPF of $\mathbf{T_i}(\lambda)$ corresponded to the in vivo SPF. The UVPE evaluation and visualization method were established using the training dataset described above.

2.4 | Practical use testing

To examine the changes in the UVPE in real-life situations, the UVPE before and after a marine leisure activity was evaluated using the MUPRIS. Moreover, to confirm the effect of any spatiotemporal decrease in the UVPE, the sunburn induced by UV irradiation from natural sunlight was recorded by an appropriate camera, and the actual sunburn state was visually evaluated by an expert. This experiment was approved by the ethical review board of Kao Corporation. Nine healthy men were selected as subjects, and four test materials were evaluated. Four test sites (10 × 9 cm for each) were prepared on each subject's back. The center of each test site was blocked from UV radiation by a silver tape. After application of the test materials, an SPF 50 + sunscreen was applied on the entire body, except on the test sites, to prevent the unpredictable sunburn. After the UV protection, the subjects spent five hours for the marine leisure activity.

During the testing procedure, the subjects were prevented from wiping and re-applying sunscreens on the test sites. The test sites were measured using the MUPRIS before application of the test materials, after the application (before the activity), at two hours after the marine leisure activity and at five hours after the activity. The average UVPE for each test site, excluding the areas with silver tapes, was calculated from the measured multispectral image. The status of the sunburn was visually evaluated the next day and compared with the UVPEs. Furthermore, multispectral UV images were captured from two healthy subjects (1 man and 1 woman) to evaluate the effect of friction on the deterioration of UV protection. The subjects applied SPF 50 + sunscreen on their entire body and spent 2 hours in marine leisure activity. The UV images for their backs were captured before and after the activity, and the UVPE changes that appeared to be caused by friction were evaluated.
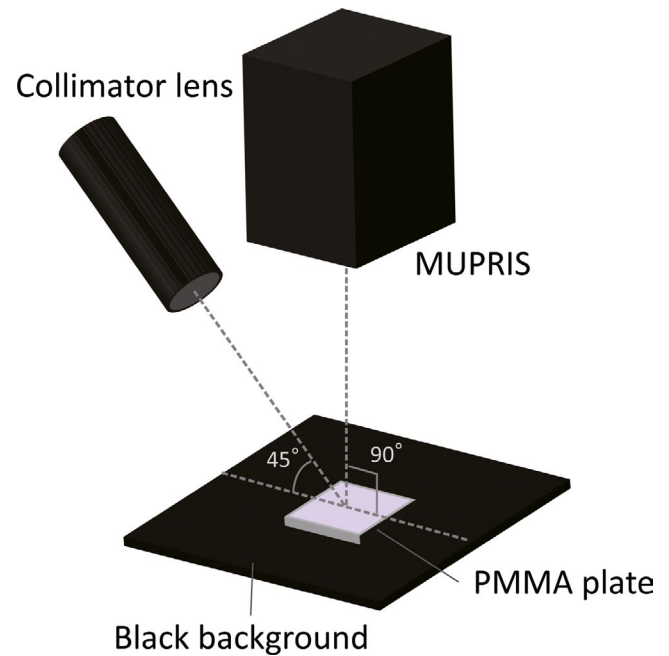
FIGURE 4 Geometry of the scattering spectra measurement [Colour figure can be viewed at wileyonlinelibrary.com]

3 | RESULTS

3.1 | MUPRIS

The MUPRIS, which can measure multispectral UV images with cross-polarization, was developed. The benefits of multispectral and polarization imaging are described in this section.

The UV images with and without polarization were captured by MUPRIS to confirm the effect of UV polarization. The results are shown in Figure 5. After applying sunscreen on half of the face, 360-nm UV images before and after toweling were captured by the MUPRIS with/ without UV polarization. Although the area with applied sunscreen was imaged darker by UV absorption, it became bright on specular light and non-observable on the UV images without polarization. In particular, the remaining sunscreen after toweling was only seen on the UV image with polarization. This implied that the presence of specular reflection light can be a serious problem when evaluating a sunscreen by a UV imaging technique, and our novel system MUPRIS perfectly solved this problem.

Before toweling   After toweling

Without polarization
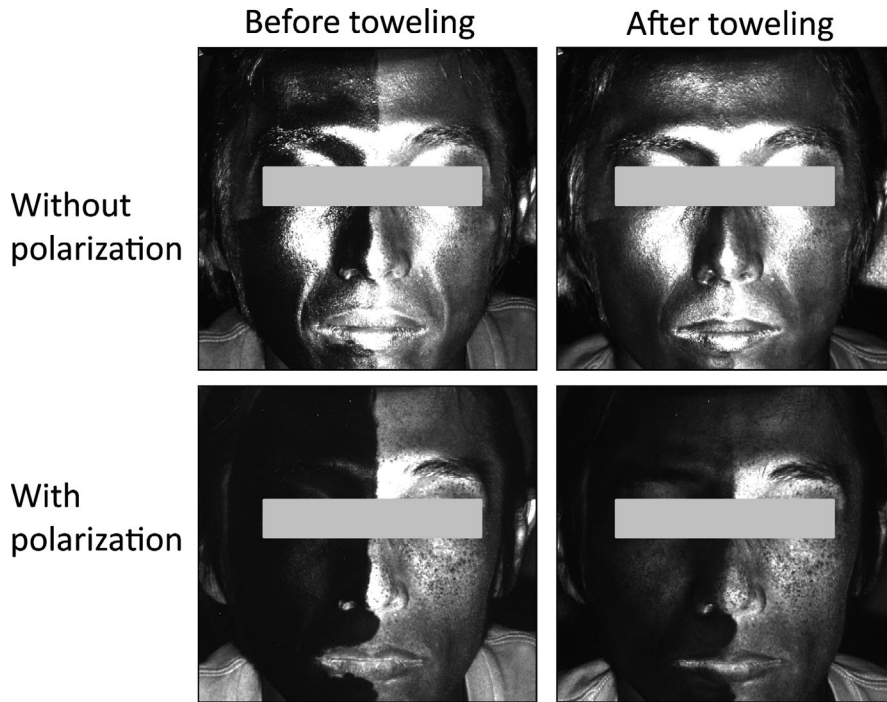
With polarization

FIGURE 5 Comparison of the UV images with and without polarization

320 nm   380 nm

UV absorbance
High
Low
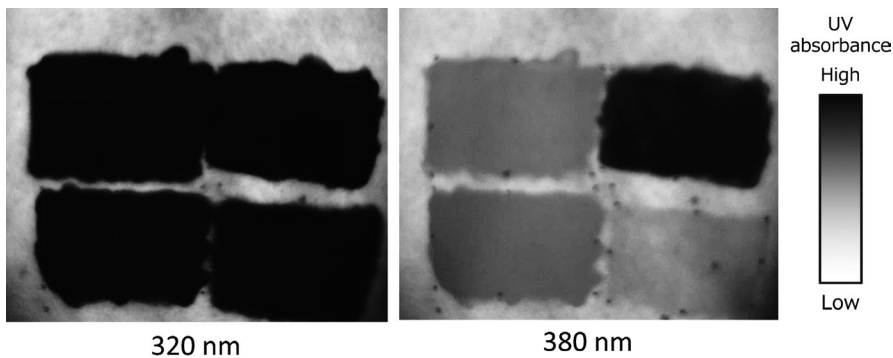
FIGURE 6 Comparison of UV images at 320 and 380 nm

Figure 6 shows the UV images captured at 320 and 380 nm. Four different test materials were applied on the square-shaped test sites. All test materials had good absorption properties on UVB but not on the UVA image. The UV scattering by inorganic UV actives (eg, zinc oxide and titanium dioxide) was probably one of the biggest causes of this difference. These inorganic UV actives have high scattering properties at a UVA wavelength range and high UV absorption properties at a UVB wavelength range.[26,27] Therefore, the materials that contained much inorganic UV actives (ie, two test sites on the left in Figure 6) were brighter at 380 nm. This is a usual case but serious problem for monitoring of UVPE. Moreover, most of the conventional UV cameras can only capture UVA images. Our system MUPRIS solved this problem and can evaluate the entire UV spectral characteristics from UVB to UVA. This multispectral image can be quite beneficial for UVPE monitoring.

The total measurement time for scanning the entire wavelength and its total UV exposure depended on the size of the test site. If the size of test site was 30 × 30 cm, UV light irradiation was added for this site and required a total exposure time of 70 seconds

(30 seconds for 310 nm, 15 seconds for 320 nm, and < 10 seconds for the other wavelengths). The total erythema-weighted UV dose was 0.02 mJ/cm^2, which was far less than the relevant dose for any outdoor condition. This implied that multispectral image measurement by the MUPRIS can be considered as noninvasive.

3.2 | UVPE estimation for the training dataset

The training dataset for the establishment of the UVPE estimation method was measured, and the accuracies of UVPE estimation of Equation (4) were evaluated. First, the UVPE estimated by Equation (4) is described in Figure 7A,B; the broken lines correspond to the point where UVPE was equal to the in vivo SPF. Equation (4) was based on the simple two layers model that was used by earlier studies. However, as can be seen in Figure 7A, all of the estimated UVPEs were significantly lower than the in vivo SPF values, regardless of the test material characteristics, such as emulsion type, form, and in vivo SPF of the test material. This result indicated that the actual sunscreen membrane was not as simple as the optical model, and

there were probably other factors that increased the reflection light. One of the reasonable hypotheses is the change in the light path length by penetration. As shown in Figure 7B, the gamma correction parameter solved this problem and almost all plots were near the broken line. However, some test materials had lower UVPE than SPF. We suspected that this was caused by the scattering effect of the test material.

To confirm the relationship between in vivo SPF estimation errors and the scattering reflection, SPF estimation error ratios were calculated and compared with the relative scattering reflectance and scatter/ transmission ratio at 320 nm (Figure 8A,B). The scatter/ transmission ratio showed good correlation with the SPF estimation error. This result indicated that scattering was one of the biggest causes of SPF estimation error and that the scatter/ transmission ratio $S_C(\lambda)$ was a reasonable correction parameter.

Using the $S_{Ci}(\lambda)$, the other correction coefficients in Equation (6) were optimized, and the UVPE for the training dataset was computed.
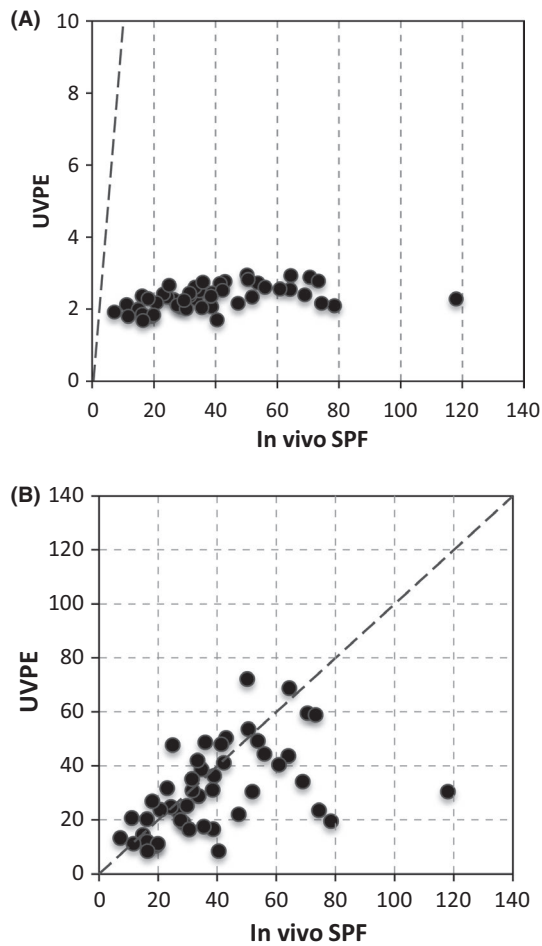
FIGURE 7 Relationship between in vivo sun protection factor (SPF) and UVPE by Equation (4). Relationship between in vivo SPF and UVPE on (A) the simple optical model (Equation (4)) and (B) after gamma correction (Equation (4)) to account for the scattering effect by the penetration of the test material into the skin. Simple optical model. B, Gamma correction considering the penetration
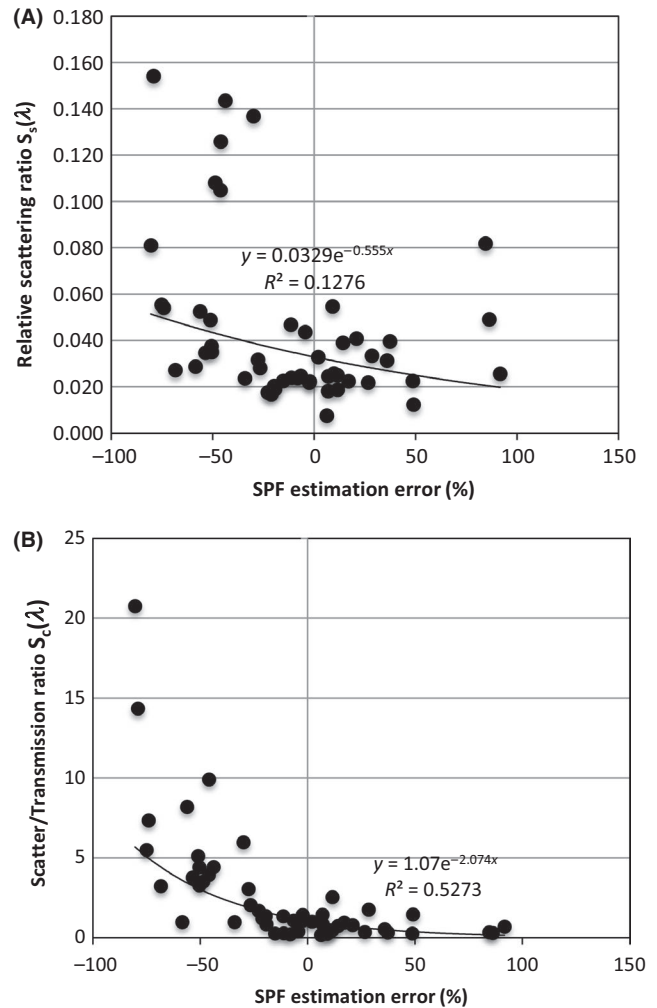
FIGURE 8 Relationships between SPF estimation error and scattering-related parameters. Scattering ratio (A) and scatter/ transmission ratio (B) were compared with the error. (A) Scattering ratio. (B) Scatter/ transmission ratio

As shown in Figure 9, the estimation accuracy was significantly improved by the scattering correction. As an example, the estimated transmittance spectra and the theoretical transmittance spectrum of test material 18 were plotted. This test material had a high scattering property for entire wavelength, because the item category was makeup foundation and it contained much titanium dioxide, zinc oxide, and pigments. As shown in Figure 10, the transmittance estimation error was perfectly eliminated by the proposed scattering correction method.

Table 2 describes the Pearson's product-moment correlation coefficients and the SEPs of the SPFs in Equation (5) for three UVPE estimation equations. The gamma correction in Equation (4) significantly improved the SEP from the simple optical model, but the correlation coefficient was not improved. The extended Equation (4), which considered the scattering effects of the test materials, improved both the correlation coefficient and the SEP from Equation (4). This result indicated that the MUPRIS with the established UVPE estimation method had sufficient SPF estimation accuracy for the evaluation of sunscreens in real-life situations.
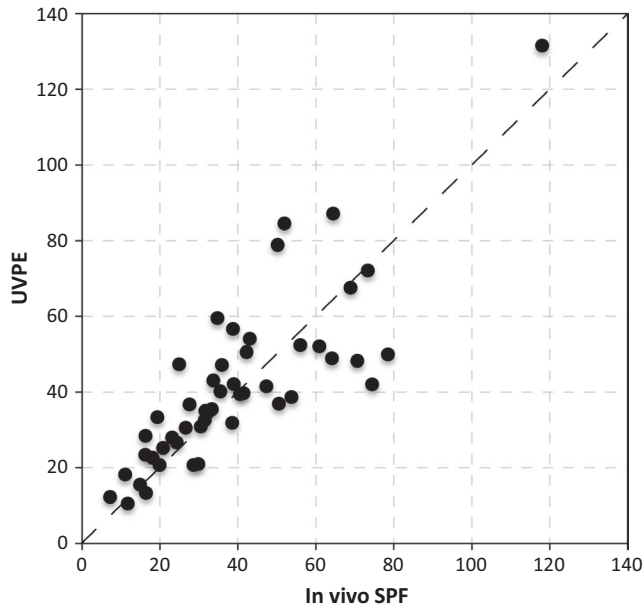
FIGURE 9 Relationship between UVPE by the scattering correction method [Equation (4)] and in vivo SPF
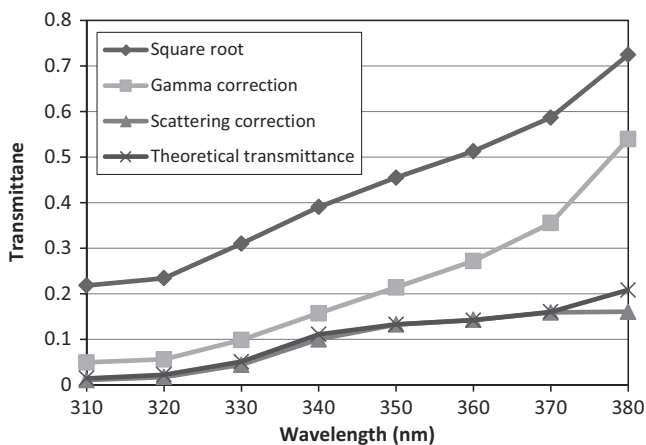
FIGURE 10 Comparison of the estimated transmittance spectra

3.3 | Practical use testing

Figure 11 illustrates the UVPE measured over time by this system and the sunburn images measured by an appropriate camera. The changing strength of the UVPE is displayed by the color bar from red (high) to blue (low). The color of the entire UV image after sunscreen application was red, but it changed to yellow or green after two

hours of marine leisure activity. After five hours, the color of the partial UV image changed to blue and the area with sunburn was largely congruent with the area that had decreased UVPE (Figure 12).

The mean values of the UVPE of each test material before and after the activity are shown in Figure 13. The left bars show the in vivo SPF values of the test materials measured in the external laboratory. The estimated UVPE values at 0 hour were approximately same as the in vivo SPFs. The UVPE of each test material clearly decreased after the marine leisure activity. At 0 hour, the UVPE values of test materials Q and R were lower than those of the others. However, only the test material Q showed lower UVPE after two hours of activity. Finally, after five hours of activity, the test material S showed the highest UVPE. To compare the monitored changes in the UVPE with the actual sunburn, we evaluated visual erythema scores on the next day and visual darkening scores after a week (Figure 14A,B). Compared with the others, the test material Q showed significantly higher scores on both erythema and darkening. This tendency was similar for the UVPE after two hours of activity. Notably, the UVPE after two hours of activity was measured at high noon; therefore, these represented the UVPEs when exposed to the highest UV irradiation, which might have caused the sunburn in the subjects. These results indicated that our novel quantitative UVPE monitoring system can be a powerful tool for the investigation of sunscreen and sunburn in real-life situations.

Figures 15 and 16 show the UV images of the cases that were demonstrated to have actual UVPE decrease in this experiment. In one subject, the UVPE decreased to only 36% after reclining on a chair, as clearly demonstrated by removal of the sunscreen film along the pattern of the back of chair (Figure 15). In the other subject, the UVPE was decreased to only 7.5% by friction against the string of the swimming wear, as clearly demonstrated by removal of the sunscreen film around the string (Figure 16). The UVPE decrease was similar or higher by friction than by 2 hours of marine leisure activity (Figure 13). This implied that friction may be one of the biggest causes of sunscreen deterioration, and maintenance of the UVPE despite friction is important to prevent harmful UV exposure.

4 | DISCUSSION

4.1 | Measurement wavelength range

In this study, a highly sensitive multispectral polarization UV imaging system was developed and a UVPE evaluation method was established to enable quantitative spatiotemporal evaluation of sunscreens in the

Model	Correction method	Equation (4)	Correlation coefficient	SEP
Simple optical model	Square root	$\sqrt{\mathbf{R}_{ri}(\lambda)}$	0.45	42.8
With penetration	Gamma correction	$\{\mathbf{R}_{ri}(\lambda)\}^{\gamma_b}$	0.49	21.2
With scattering	Scattering correction	$\{\mathbf{R}_{ri}(\lambda)\}^{\gamma_{si}(\lambda)}$	0.82	13.3

TABLE 2 Comparison of the in vivo SPF estimation accuracies
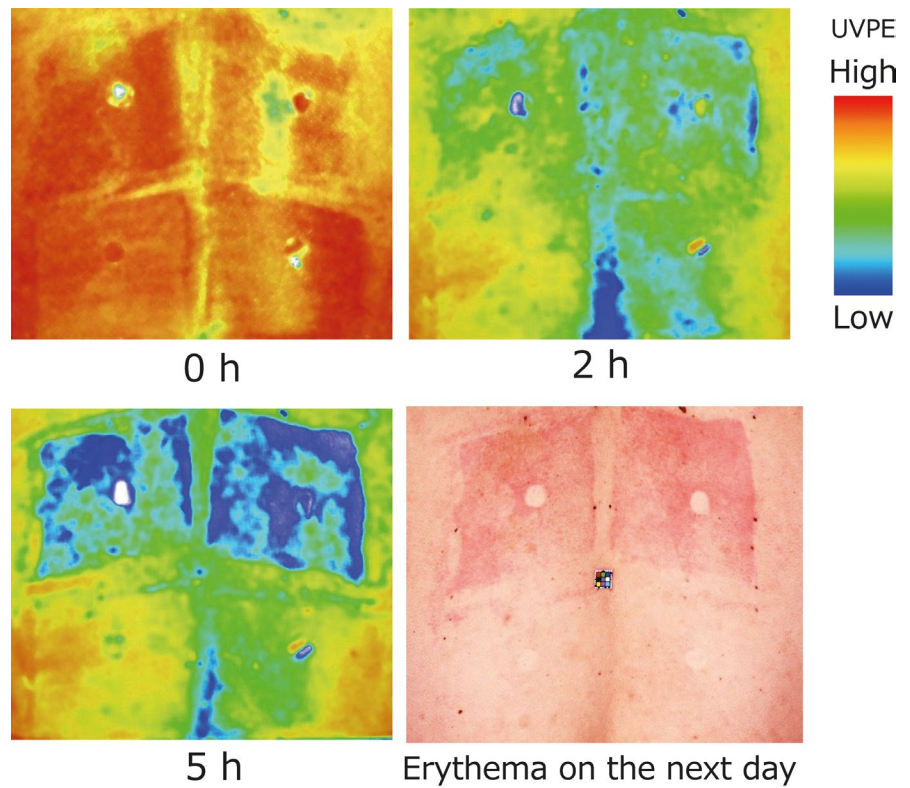
FIGURE 11 UVPE monitoring results and a photograph of the erythema the next day
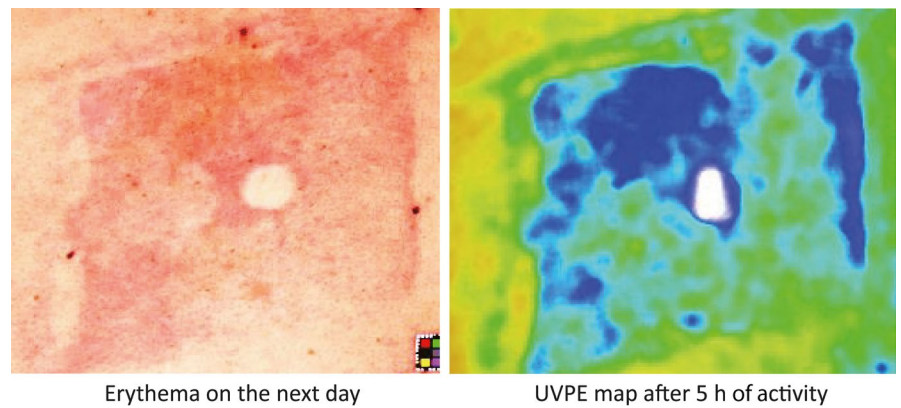
FIGURE 12 Comparison of the patterns of erythema and UVPE
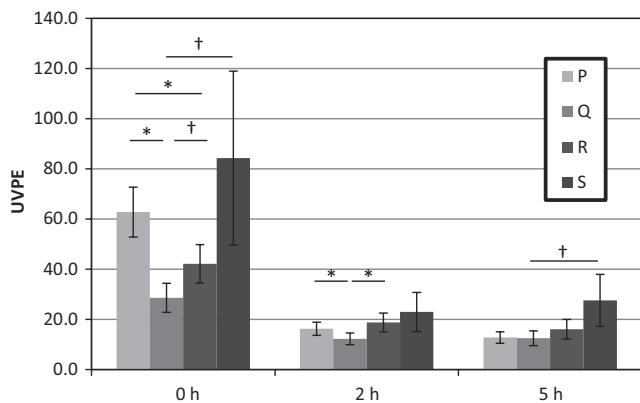
FIGURE 13 Changes in the UVPE during marine leisure activity. The bars on the left show the in vivo SPF values of the test materials measured by the external laboratory. The error bars represent the standard errors. *$P < 0.05$, †$P < 0.1$ by the paired t test

real-world setting. The UVPE can be calculated by Equation (1) using the in vitro SPF method. Although transmittance between 290 and 400 nm is used to calculate the in vitro SPF, our UVPE calculation using a transmittance of 310-380 nm showed good correlation with in vivo SPF. The reason for this result was that the most effective wavelength for sunburn was around 310 nm, which was calculated by multiplying the erythema action spectrum $E(\lambda)$ with the spectrum of UV light $I_s(\lambda)$ (Figure 17). In addition, most of the UV filters have broad absorption spectral characteristics. Therefore, the absorption of missing wavelength ranges may correlate with the absorption at 310 nm, and a drop in the estimated value was considered to be low.

4.2 | Comparison with DRS methods

Our UVPE estimation method was different from the earlier reported DRS methods,[21-23] although it also aimed to estimate transmittance from the diffuse reflectance spectra. The differences are discussed

(A)

(B)
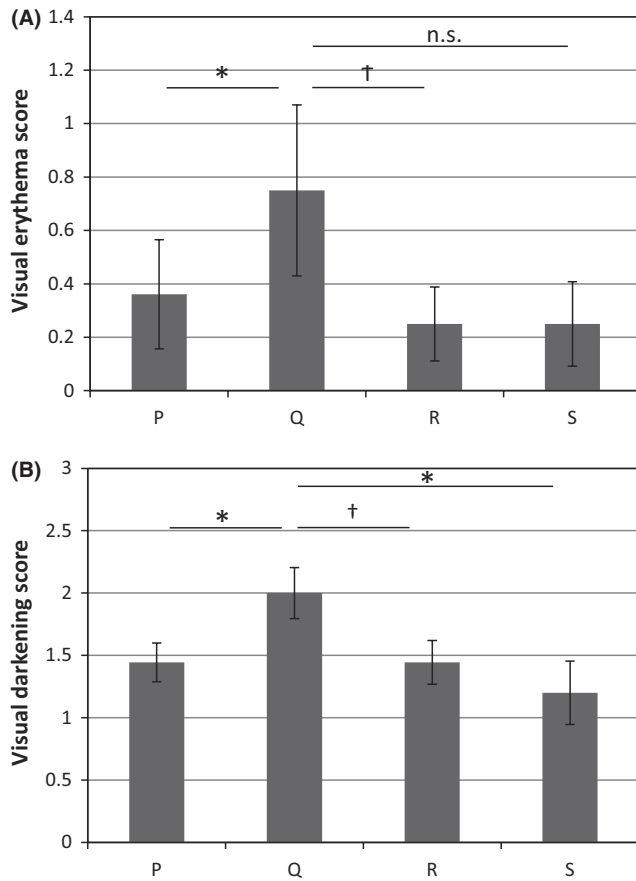
FIGURE 14 Visual evaluation of erythema on the next day and darkening after a week. The mean values are plotted, and the standard errors are described as the error bars. Student's *t* test was used for statistical analysis. ns, not significant; †$P < 0.1$; *$P < 0.05$. A, Erythema on the next day. B, Darkening after a week

FIGURE 16 Decrease in the UVPE by friction against the string of a swimming wear. The upper image shows a photograph taken by a conventional RGB camera. The bottom image shows the UV image at 340 nm [Colour figure can be viewed at wileyonlinelibrary.com]

in this section. As described in the results, we introduced the spectral correction parameter $\gamma_{si}(\lambda)$ to improve the SPF estimation accuracy. However, earlier studies that used only the simple optical model showed good estimation accuracies without such correction; this was probably caused by the differences in the measurement devices, especially the detector. Earlier studies used a fiber probe with illumination and detection fibers to measure a reflectance spectrum by contact with the test site. With this measurement setting, the internal

scattering light from skin can be measured as the reflection and was robust for the scattering effect of the sunscreen on the skin. Therefore, they did not need to introduce the scattering correction parameter. On the other hand, we used UV camera as a detector, because a noncontact measurement method was required for in situ monitoring. Because of noncontact measurement, the MUPRIS may contain more scattering light component of the reflectance spectra, compared with that of the earlier contact measurement method. Therefore, our approach of correcting the spectra based on a premeasured scattering spectrum was probably a reasonable way to estimate the transmittance spectrum of the sunscreen; in fact, it improved the estimation accuracy of spatiotemporal measurement. Meanwhile, the estimated UVPE by the MUPRIS can be strongly affected by individual typology angle values,[28] because the effect of scattering on the relative reflectance will be higher for dark skin than for light skin. Calibration of the gamma correction parameter for each subject may be effective in decreasing this intersubject variance.

Rohr et al showed that spectral correction according to the photostability of a test material significantly improved the SPF estimation accuracy.[23] However, in this study, we did not include this
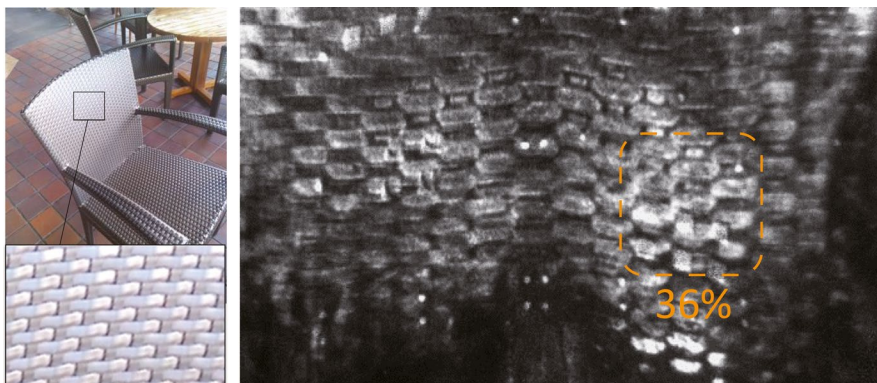
FIGURE 15 Decrease in the UVPE by reclining on a chair. The images on the left show the reclined chair, and image on the right shows the 340-nm UV image captured after reclining [Colour figure can be viewed at wileyonlinelibrary.com]
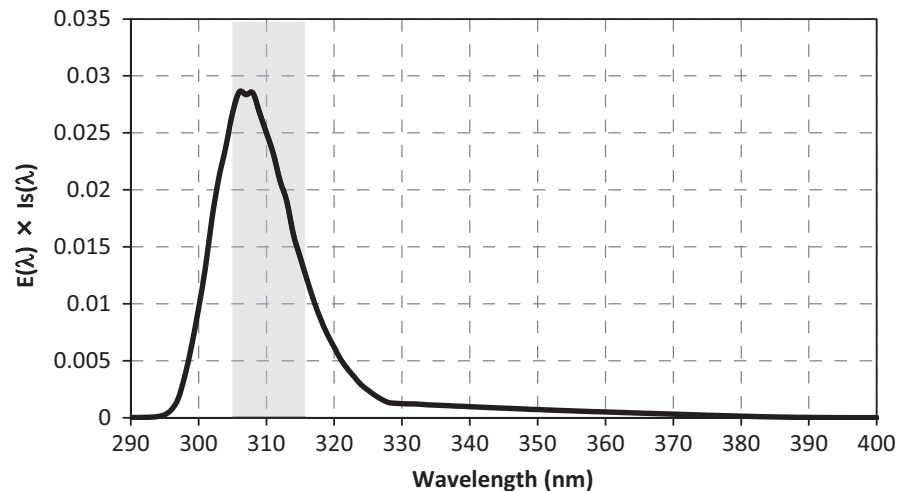
FIGURE 17 Multiplication of the erythema action spectrum with the UV irradiation. The shaded region represents the transmission range of the band-pass filter at 310 nm

process in our UVPE estimation algorithm, because our system aimed to monitor the in situ UVPE. If the test material was not photostable, the UVPE should decrease along with UV exposure, and such temporal change should be monitored by our system. The effect of photostability on in vivo SPF was one limitation of our system for SPF estimation accuracy.

4.3 | Application for behavioral investigations

Several behavioral investigations on sun protection and UV exposure of consumers in real-life situations have been reported earlier. The potential application of our novel system for such investigations is discussed in this section.

There were several behavioral studies on sunscreen use that aimed to identify the difference between theoretical UVPE (ie, labeled SPF) and actual UV protection and to find out ways to improve UV protection.[8-13,29-40] Most of those studies showed that the amount of applied sunscreen in real-life situations was significantly lower than the amount defined in the ISO24444. The reported amounts varied from 0.1 to 1.6 mg/cm^2, and this was probably caused by the formulations used, the situations, countries, examined areas, and weighing methods.[12,13,29,30] However, the actual UVPEs were unknown, because there were several different reports about the relationship between the in vivo SPF and applied amount.[36,37] In some behavioral studies, conventional UV camera or fluorescent ingredients in specific sunscreens were used for the visualization and quantification of the applied sunscreen.[13,24,30] Compared with conventional imaging techniques, MUPRIS does not provide the total applied amount of sunscreen, but it can precisely provide the actual and real-time UVPE within a few minutes. Therefore, MUPRIS may allow larger and in-depth investigations in this research field.

Studies on the degradation of UVPE are fewer than the investigations on the applied amount of sunscreen. Whiteman et al reported on the decrease in the absorbance of swabbed sunscreen during two hours of activity.[10] However, O'riordan et al and Bauer et al pointed out that the absorbance of sunscreen was also affected, even with the lack of swab.[11,12] As mentioned in the introduction, some studies

on UVPE degradation were based on the in vivo SPF testing.[8,9] However, the inherent problems of the in vivo SPF method can make it difficult to attempt scale expansion by inclusion of varied products and activities and a large number of subjects. The MUPRIS can be a powerful tool to solve this problem and can allow large-scale investigation to clarify the degradation of the UVPE in real-life situations.

5 | CONCLUSION

In this study, a highly sensitive multispectral polarization UV imaging system was developed together with a UVPE estimation algorithm. The estimated UVPE showed good correlation with in vivo SPF measurements. Moreover, this system succeeded in spatiotemporal evaluations of the UVPE in real-life situations; in particular, a sunscreen UVPE can be strongly influenced by the degree of sunburn that subsequently occurs after its application on the skin. In addition, we found the physical friction was quite a serious UVPE degradation factor. In our future work, we are going to apply MUPRIS on a large variety of behavioral studies to approximate the actual causes of sunburn in the real-life setting and to evaluate the actual efficacy of sunscreen products. We believe that this will help in the development of innovative sunscreen products that can perfectly protect against UV irradiation in real-life situations.

CONFLICT OF INTEREST

There are no conflicts of interest to declare.

ORCID

Ken Nishino [iD] https://orcid.org/0000-0002-0660-2972

REFERENCES

1. D'Orazio J, Jarrett S, Amaro-Ortiz A, Scott T. UV radiation and the skin. *Int J Mol Sci*. 2013;14(6):12222-12248.

2. Łastowiecka-Moras E, Bugajska J, Młynarczyk B. Occupational exposure to natural UV radiation and premature skin ageing. *Int J Occup Saf Ergon*. 2014;20(4):639-645.

3. Imokawa G. Recent advances in characterizing biological mechanisms underlying UV-induced wrinkles: a pivotal role of fibroblast-derived elastase. *Arch Dermatol Res*. 2008;300(1):7-20.

4. Gilchrest BA, Park H-Y, Eller MS, Yaar M. Mechanisms of ultraviolet light-induced pigmentation. *Photochem Photobiol*. 1996;63(1):1-10.

5. International Standard ISO 24444. Cosmetics – sun protection test methods – in vivo determination of the sun protection factor (SPF), 1st edn, 2010. www.iso.org

6. Petersen B, Wulf HC. Application of sunscreen – theory and reality. *Photodermatol Photoimmunol Photomed*. 2014;30(2–3):96-101.

7. COLIPA. Guidelines for evaluating sun product water resistance. 2005. https://www.cosmeticseurope.eu

8. Beyer DM, Faurschou A, Haedersdal M, Wulf HC. Clothing reduces the sun protection factor of sunscreens. *Br J Dermatol*. 2010;162(2):415-419.

9. Bodekær M, Faurschou A, Philipsen PA, Wulf HC. Sun protection factor persistence during a day with physical activity and bathing. *Photodermatol Photoimmunol Photomed*. 2008;24(6):296-300.

10. Whiteman DC, Brown RM, Xu C, Paterson CL, Miller D, Parsons PG. A rapid method for determining recent sunscreen use in field studies. *J Photochem Photobiol B Biol*. 2003;69(1):59-63.

11. O'Riordan DL, Lunde KB, Urschitz J, Glanz K. A noninvasive objective measure of sunscreen use and reapplication. *Cancer Epidemiol Prev Biomarkers*. 2005;14(3):722-726.

12. Bauer U, O'Brien DS, Kimlin MG. A new method to quantify the application thickness of sunscreen on skin. *Photochem Photobiol*. 2010;86(6):1397-1403.

13. Lademann J, Schanzer S, Richter H, et al. Sunscreen application at the beach. *J Cosmet Dermatol*. 2004;3(2):62-68.

14. Sauermann G, Hoppe U. A rapid non-injurious method to evaluate the light protective potential of sunscreens. *J Soc Cosmet Chem*. 1985;36:125-141.

15. Azurdia RM, Pagliaro JA, Diffey BL, Rhodes LE. Sunscreen application by photosensitive patients is inadequate for protection. *Br J Dermatol*. 1999;140(2):255-258.

16. Rhodes LE, Diffey BL. Quantitative assessment of sunscreen application technique by in vivo fluorescence spectroscopy. *J Soc Cosmet Chem*. 1996;47(2):109-115.

17. Utz SR, Knuschke P, Sinichkin YP. Optical and imaging techniques for in-vivo sunscreens investigation. *Barcelona-DL Tentative*. 1996;323-333.

18. Miksa S, Lutz D, Guy C, Delamour E. New approach for a reliable in vitro sun protection factor method–Part II: practical aspects and implementations. *Int J Cosmet Sci*. 2016;38(5):504-511.

19. Pissavini M, Tricaud C, Wiener G, et al. Validation of an in vitro sun protection factor (SPF) method in blinded ring-testing. *Int J Cosmet Sci*. 2018;40(3):263-268.

20. Miura Y, Takiguchi Y, Shirao M, et al. Algorithm for in vitro sun protection factor based on transmission spectrum measurement with concomitant evaluation of photostability. *Photochem Photobiol*. 2008;84(6):1569-1575.

21. Reble C, Gersonde I, Schanzer S, Meinke MC, Helfmann J, Lademann J. Evaluation of detection distance-dependent reflectance spectroscopy for the determination of the sun protection factor using pig ear skin. *J Biophotonics*. 2018;11(1):e201600257-e201600257.

22. Ruvolo Junior E, Kollias N, Cole C. New noninvasive approach assessing in vivo sun protection factor (SPF) using diffuse reflectance spectroscopy (DRS) and in vitro transmission. *Photodermatol Photoimmunol Photomed*. 2014;30(4):202-211.

23. Rohr M, Ernst N, Schrader A. Hybrid diffuse reflectance spectroscopy: non-erythemal in vivo testing of sun protection factor. *Skin Pharmacol Physiol*. 2018;31(4):220-228.

24. Jovanovic Z, Schornstein T, Sutor A, Neufang G, Hagens R. Conventional sunscreen application does not lead to sufficient body coverage. *Int J Cosmet Sci*. 2017;39(5):550-555.

25. Mahler H, Kulik JA, Harrell J, Correa A, Gibbons FX, Gerrard M. Effects of UV photographs, photoaging information, and use of sunless tanning lotion on sun protection behaviors. *Arch Dermatol*. 2005;141(3):373-380.

26. Becheri A, Dürr M, Lo NP, Baglioni P. Synthesis and characterization of zinc oxide nanoparticles: application to textiles as UV-absorbers. *J Nanoparticle Res*. 2008;10(4):679-689.

27. Reddy KM, Manorama SV, Reddy AR. Bandgap studies on anatase titanium dioxide nanoparticles. *Mater Chem Phys*. 2003;78(1):239-245.

28. Chardon A, Cretois I, Hourseau C. Skin color typology and suntanning pathways. *Int J Cosmet Sci*. 1991;13(4):191-208.

29. Autier P, Boniol M, Severi G, Dore J-F, Research EOF, Group TOCMC-O. Quantity of sunscreen used by European students. *Br J Dermatol*. 2001;144(2):288-291.

30. Heerfordt IM. Sunscreen use at Danish beaches and how to improve coverage. *Dan Med J*. 2018;65(4):1-13.

31. Bech-Thomsen N, Wulf HC. Sunbathers' application of sunscreen is probably inadequate to obtain the sun protection factor assigned to the preparation. *Photodermatol Photoimmunol Photomed*. 1992;9(6):242-244.

32. Neale R, Williams G, Green A. Application patterns among participants randomized to daily sunscreen use in a skin cancer prevention trial. *Arch Dermatol*. 2002;138(10):1319-1325.

33. Novick R, Anderson G, Miller E, Allgeier D, Unice K. Factors that influence sunscreen application thickness and potential preservative exposure. *Photodermatol Photoimmunol Photomed*. 2015;31(4):212-223.

34. Szepietowski JC, Nowicka D, Reich A, Melon M. Application of sunscreen preparations among young Polish people. *J Cosmet Dermatol*. 2004;3(2):69-72.

35. Petersen B, Datta P, Philipsen PA, Wulf HC. Sunscreen use and failures–on site observations on a sun-holiday. *Photochem Photobiol Sci*. 2013;12(1):190-196.

36. Teramura T, Mizuno M, Asano H, Naito N, Arakane K, Miyachi Y. Relationship between sun-protection factor and application thickness in high-performance sunscreen: double application of sunscreen is recommended. *Clin Exp Dermatol*. 2012;37(8):904-908.

37. Liu W, Wang X, Lai W, et al. Sunburn protection as a function of sunscreen application thickness differs between high and low SPFs. *Photodermatol Photoimmunol Photomed*. 2012;28(3):120-126.

38. Kim SM, Oh BH, Lee YW, Choe YB, Ahn KJ. The relation between the amount of sunscreen applied and the sun protection factor in Asian skin. *J Am Acad Dermatol*. 2010;62(2):218-222.

39. Schalka S, Dos Reis V, Cucé LC. The influence of the amount of sunscreen applied and its sun protection factor (SPF): evaluation of two sunscreens including the same ingredients at different concentrations. *Photodermatol Photoimmunol Photomed*. 2009;25(4):175-180.

40. Ou-Yang H, Stanfield J, Cole C, Appa Y, Rigel D. High-SPF sunscreens (SPF≥70) may provide ultraviolet protection above minimal recommended levels by adequately compensating for lower sunscreen user application amounts. *J Am Acad Dermatol*. 2012;67(6):1220-1227.